MULTIPION PRODUCTION WITH SIMULTANEOUS EXCITATION OF DISCRETE NUCLEAR LEVELS

By H. Leśniak and L. Leśniak

Institute of Nuclear Physics, Cracow*

(Received March 26, 1974)

Production processes of multihadron systems leading to the excitation of the discrete nuclear levels are studied in the framework of the distorted wave impulse approximation model. The influence of the nuclear absorption of the outgoing multiparticle system on the effective mass and momentum transfer distributions is examined. Amplitudes for the process $\pi^{12}C \to \pi\pi\pi^{12}C^*$ (4.4 MeV) are derived and the results compared with experimental data.

1. Introduction

Multiparticle production has been extensively studied in the coherent processes on nuclei [1]. Identification of the coherent events requires a separation of the nuclear ground state from the excited states. This is very difficult to achieve using high energy hadron beams. However, the fact that angular distributions of the coherently produced multihadron states are very sharply peaked in the *forward* direction and dominate over the incoherent production differential cross sections, helps in isolation of the coherent events (see for example Ref. [2]). This experimental procedure cannot be used in studying the multiparticle production with simultaneous excitation of some final nuclear state. Therefore a new experimental technique has been developed in which one detects photons emitted by excited nuclei. This technique was applied by two experimental groups working at Berkeley and Argonne in the study of the inelastic pion scattering [3, 4] and the coherent three pion production [5]:

$$\pi^{-12}\mathrm{C} \to \pi^+\pi^-\pi^{-12}\mathrm{C}^* \ (4.4\ \mathrm{MeV}). \tag{1}$$

The 4.4 MeV level of ^{12}C has isospin $T = 0$ and spin parity 2^+ therefore only isospin zero can be exchanged in the t-channel of reaction (1).

Choosing experimentally different excited states of the nucleus makes possible the application of the isospin and spin-parity selection rules which may help to obtain various parts of the production amplitude on *nucleons*. Such selection rules have been discussed

* Address: Instytut Fizyki Jądrowej, Radzikowskiego 152, 31-342 Kraków 23, Poland.

by Stodolsky [6] in the distorted wave impulse approximation model (DWIA). In this model one assumes that the production and the nuclear excitation process takes place on a single target nucleon, while the remaining nucleons scatter elastically the incoming and outgoing particles. The DWIA model has been applied to the description of the inelastic scattering of pions on carbon [4, 7, 8]. Proton inelastic scattering on different nuclei was also studied in Refs [9–14] and reviewed in Ref. [15].

The distorted wave impulse approximation may be considered as a special limit of the Glauber multiple collision model [16]. The assumption that the transition has a direct character (one-step process) plays here a crucial role [7, 10, 14]. The Glauber model has been successfully applied to the description of the high-energy elastic and inelastic hadron scattering from nuclei [17]. It has been further extended to the analysis of the particle production in nuclei [18] and has yielded very important information about the interaction of the unstable particles (resonances) and group of hadrons (for example three- or five-pion systems) with nucleons [2, 19, 20]. Almost all the experimental data suggest that the absorption of multihadron systems in nuclei is the same as that of the single hadron; for example the total cross sections of 3π or 5π systems on nucleons are of the same order as the pion-nucleon total cross section. Experiments on the production of resonance on nuclei provided a similar conclusion, though this fact was expected. Recently a preliminary spin-parity analysis of the 3π system produced coherently on a variety of nuclei yielded some evidence that the 0^- final state is absorbed in nuclei about *twice as strongly* as the incoming pion [21]. If this observation is confirmed, the present theoretical attempts to explain the low absorption of the multiparticle systems in nuclear matter will have to be modified.

In the production processes with the excitation of the final nucleus as in the reaction (1) the problem of the absorption of the outgoing hadron system appears similarly as in the coherent production process. Therefore these reactions may serve as an independent source of information on the propagation of hadronic states through nuclear matter. Our present experimental information about these processes is still very scanty, hence in the present paper we shall use a simple model to describe them. The model is presented in Sect. 2. In Sect. 3 we derive the amplitudes for the process (1). Sect 4 contains an application of the model to the analysis of experimental data of Ref. [5], and conclusions are summarized in Sect. 5.

2. *The model*

The model used here is essentially the distorted wave impulse approximation model. We can apply it to the following high-energy reaction

$$1+A \to 2+A^*, \tag{2}$$

where 1 denotes the projectile particle, A is the target nucleus in the ground state, 2 is the outgoing particle or group of particles produced in coincidence with an excitation of the discrete nuclear level.

Before writing the final formula we shall pass a set of intermediate steps showing

a link of the DWIA with the Glauber model and serving also as an explanation of the assumptions needed in the DWIA model. The main assumption of the model is that the cross section of the production process on the nucleon N

$$1+\mathrm{N} \to 2+\mathrm{N} \tag{3}$$

is much smaller than the elastic cross section for the scattering of particles 1 or 2 on the nucleon. Then, similarly to the amplitude for the coherent production process (cf. Ref. [18]) the amplitude of the process (2) is given by

$$T(\vec{q}) = \frac{ip}{2\pi} \int d^2b e^{i\vec{q}_\mathrm{T}\vec{b}} \sum_{j=1}^{A} \int d^3r_1 \ldots d^3r_A \Psi_\mathrm{f}^*(\vec{r}_1 \ldots \vec{r}_A) \times$$

$$\times \prod_{k\neq j} [1-\gamma_{22}(\vec{b}-\vec{s}_k)\theta(z_k-z_j)]\gamma_{12}(\vec{b}-\vec{s}_j)e^{iq_\mathrm{L}z_j} \prod_{i\neq j} [1-\gamma_{11}(\vec{b}-\vec{s}_i)\theta(z_j-z_i)]\Psi_i(\vec{r}_1 \ldots \vec{r}_A), \tag{4}$$

where p is the incoming particle momentum, $\vec{q}_\mathrm{T}$ and q_L are transverse and longitudinal components of the momentum transfer $\vec{q}$, $\Psi_f(\vec{r}_1 \ldots \vec{r}_A)$ and $\Psi_i(\vec{r}_1 \ldots \vec{r}_A)$ are the final and initial (ground state) wave functions. The vector $\vec{b}$ is the impact parameter vector and $\vec{s}_j$ is the position vector of the j-the target nucleon in the plane perpendicular to the momentum $\vec{p}$ chosen along the z-axis. The functions γ_{12}, γ_{11} and γ_{22} are the profile functions related to the production amplitude $f_{12}(q)$ and the elastic scattering amplitudes $f_{11}(q)$ and $f_{22}(q)$ of particles 1 and 2 on the nucleon. This relation is the following Fourier-Bessel transform:

$$\gamma_{xy}(b) = \frac{1}{2\pi ip} \int d^2q f_{xy}(q) e^{-i\vec{q}\vec{b}}, \tag{5}$$

where $\vec{q}$ is the momentum transfer and $x, y = 1, 2$. The ordering of functions γ_{xy} in Eq. (4) given by the step functions $\theta(z)$ means that the particle 1 first scatters elastically on a certain number of target nucleons having z_i-coordinates smaller than z_j, then produces the particle 2 on the j-th nucleon, and finally scatters elastically on the nucleons having the z_k coordinates greater than z_j. When more than one particle is produced on the j-th nucleon we treat the scattering of the whole system in the same manner as the scattering of a single particle.

The amplitudes f_{11}, f_{22}, and f_{12} may be treated as operators acting in the target nucleon spin and isospin space. In order to simplify our considerations we neglect the nucleon spin-flip parts of these amplitudes and their dependence on the spins of incoming and produced particles. Because at high energies the interactions of hadrons with proton and neutron are very similar, we take only the isoscalar parts of the *elastic* scattering amplitudes f_{11} and f_{22}, which means that we use averages of the proton and neutron amplitudes. When calculating the reaction (2) amplitude we use the isospin selection rules, choosing the appropriate isospin parts of the *production* amplitude f_{12}. For example, in the process (1) only the isoscalar part of this amplitude can participate. When the final

nuclear state has isospin 1 while the ground state has isospin 0, only the isovector amplitude contributes to the process.

Evaluation of the transition matrix element (4) needs a detailed knowledge of the initial and final state wave functions. At this point we have to choose some models of these wave functions. In the calculations of the elastic scattering or the coherent production processes on nuclei the following approximation is often made:

$$\Psi_i^*(\vec{r}_1, \ldots, \vec{r}_A)\Psi_i(\vec{r}_1, \ldots, \vec{r}_A) = \prod_{j=1}^{A} \varrho(r_j), \tag{6}$$

where the single particle density in the ground state is

$$\varrho(\vec{r}_1) = \int d^3r_2 \ldots d^3r_A \Psi_i^*(\vec{r}_1, \ldots, \vec{r}_A)\Psi_i(\vec{r}_1, \ldots, \vec{r}_A). \tag{7}$$

Correspondingly we may assume that

$$\Psi_f^*(\vec{r}_1, \ldots, \vec{r}_A)\Psi_i(\vec{r}_1, \ldots, \vec{r}_A) = \sum_{j=1}^{A} \varrho_{fi}(\vec{r}_j) \prod_{k \neq j} \varrho(\vec{r}_k) \tag{8}$$

defining the transition density $\varrho_{fi}(\vec{r})$ as

$$\varrho_{fi}(\vec{r}_1) = \int d^3r_2 \ldots d^3r_A \Psi_f^*(\vec{r}_1, \ldots, \vec{r}_A)\Psi_i(\vec{r}_1, \ldots, \vec{r}_A). \tag{9}$$

In Eq. (8) we have neglected any difference between the ground and the excited state single particle density distributions and the two or more particle correlations. We assume further that the production of particle 2 and excitation of the nucleus takes place on the same j-th nucleon. In this way we get the following expression for the amplitude:

$$T(\vec{q}) = A \frac{ip}{2\pi} \int d^2b dz d^2s e^{i\vec{q}_T\vec{b}} e^{iq_L z} \varrho_{fi}(\vec{r}) \gamma_{12}(\vec{b}-\vec{s}) G(\vec{b}, z), \tag{10}$$

where the absorption factor $G(\vec{b}, z)$ is

$$G(\vec{b}, z) = [1 - \int_{-\infty}^{z} dz' \int d^2s' \varrho(\vec{s}', z')\gamma_{11}(\vec{b}-\vec{s}') -$$

$$- \int_{z}^{\infty} dz' \int d^2s' \varrho(\vec{s}', z')\gamma_{22}(\vec{b}-\vec{s}')]^{A-1}. \tag{11}$$

In the limit of large A we approximate $G(\vec{b}, z)$ as

$$G(\vec{b}, z) = \exp\{-(A-1)[\int_{-\infty}^{z} dz' \int d^2s' \varrho(\vec{s}', z')\gamma_{11}(\vec{b}-\vec{s}') +$$

$$+ \int_{z}^{\infty} dz' \int d^2s' \varrho(\vec{s}', z')\gamma_{22}(\vec{b}-\vec{s}')]\}. \tag{12}$$

Going further, we define the folded transition density distribution $\tilde{\varrho}_{fi}(\vec{b}, z)$

$$\tilde{\varrho}_{fi}(\vec{b}, z) f_{12}(0) = \frac{ip}{2\pi} \int d^2s \varrho_{fi}(\vec{s}, z)\gamma_{12}(\vec{b}-\vec{s}), \tag{13}$$

assuming that the forward production amplitude $f_{12}(0)$ differs from zero.

Finally we get

$$T(\vec{q}) = Af_{12}(0) \int d^3r e^{i\vec{q}\vec{r}} \varrho_{fi}(\vec{r}) G(\vec{r}). \tag{14}$$

Let us now discuss the case of the negligible absorption, i. e. $G(\vec{r}) \equiv 1$. This is the case of the elastic electron scattering in which the transition form factors $F_{fi}(\vec{q})$ are measured [22]. They are related to the densities $\varrho_{fi}(\vec{r})$ by means of the Fourier transform

$$F_{fi}(\vec{q}) = \int d^3r e^{i\vec{q}\vec{r}} \varrho_{fi}(\vec{r}). \tag{15}$$

Eq. (15) enables us to calculate the unknown transition densities from the electron inelastic scattering data. One should, however, remember that $\varrho_{fi}(\vec{r})$ must have a definite tensor character, being a reflection of the spin structure of the final and initial nuclear states. For example, for the transition from the zero spin ground state to the state of the spin J and its projection M the transition density has the following form

$$\varrho_{fi}(\vec{r}) = \varrho_J(r) Y^*_{JM}(\Omega_r). \tag{16}$$

Here $Y_{JM}(\Omega_r)$ denotes the spherical harmonic function and $\varrho_J(r)$ depends only on the absolute value of $\vec{r}$. The transition form factors are in this case

$$F_{fi}(\vec{q}) = F_J(q) \sqrt{\frac{4\pi}{2J+1}}\, Y^*_{JM}(\Omega_q), \tag{17}$$

$$F_J(q) = \sqrt{4\pi(2J+1)}\,(-i)^J \int_0^\infty dr r^2 \varrho_J(r) j_J(qr), \tag{18}$$

where $j_J(qr)$ is the spherical Bessel function and Ω_q is the solid angle of the momentum transfer $\vec{q}$. Inverting Eq. (18) we express the function $\varrho_J(r)$ in terms of $F_J(q)$:

$$\varrho_J(r) = i^J \pi^{-3/2} (2J+1)^{-1/2} \int_0^\infty dq q^2 F_J(q) j_J(qr). \tag{19}$$

If the form factor $F_J(q)$ is known, then using Eqs (19), (16), and (13) we can calculate the amplitude $T(\vec{q})$ given by Eq. (14). The influence of the Coulomb interactions may be included in Eq. (14) multiplying the integrand by the factor $\exp(i\chi_c(b))$; $\chi_c(b)$ being the nuclear Coulomb phase shift.

3. Derivation of the amplitude for the process $\pi + {}^{12}C \to 3\pi + {}^{12}C^*$ (4.4 MeV)

We study the 3π production process in which the 2^+(4.4 MeV) state of carbon is excited. The choice of this reaction is motivated by the existence of the preliminary data [5] of this reaction together with a set of data for the inelastic scattering of electrons, pions, and protons with the excitation of the same carbon state.

First of all we have to parametrize the amplitudes for the π-nucleon elastic scattering, 3π-nucleon elastic scattering, and the production amplitude. For the elastic scattering amplitudes we write

$$f_{ii}(q) = \frac{ip\sigma_i(1-i\alpha_i)}{4\pi} e^{-\frac{a_i}{2}q^2}, \quad i = 1, 2, \tag{20}$$

where the indices 1 and 2 stand for the π-nucleon scattering and the 3π-nucleon scattering, σ_i are the corresponding total cross section, α_i-ratios of the real to the imaginary parts of the forward elastic scattering amplitudes, and a_i denote the slopes of the angular distributions

$$\frac{d\sigma_{ii}}{d\Omega}(q) = |f_{ii}(q)|^2. \tag{21}$$

Because we intend to study the transverse momentum transfer squared and the 3π-mass distributions, the normalization of the production amplitude $f_{12}(m, q)$ for $\pi + N \to \to 3\pi + N$ reaction is as follows

$$\frac{d^2\sigma_N}{dm dq_\perp^2} = |f_{12}(m, \vec{q})|^2. \tag{22}$$

For this amplitude we assume

$$f_{12}(m, \vec{q}) = f_{12}(m, 0) e^{-\frac{a}{2}q^2}. \tag{23}$$

Such a dependence is suggested by the data [23] of the $\pi^{\pm}p \to (3\pi)^{\pm}p$ process, a slope parameter a may also depend on the 3π effective mass m.

In our phenomenological approach we utilize the electron scattering data of Ref. [24] and parametrize the inelastic form factor of ^{12}C (4.4 MeV) state as

$$F_2(q) = B_2 q^2 e^{-\frac{q^2}{4d_2^2}}, \tag{24}$$

where B_2 and d_2 are constants. Strictly speaking, in the evaluation of the parameter d_2 we must take into account the proton electromagnetic form factor $F_p(q)$; moreover a correction factor for the centre-of-mass motion of ^{12}C is also needed. In the analysis [25] of the elastic proton scattering from carbon this factor has a simple form, $F_{CM} = \exp(q^2/48 d_2^2)$, which we adopt here. When comparing our parametrization with the electron data, we multiply the form factor $F_2(q)$ by the proton form factor $F_p = \exp(1/6 \langle r_p^2 \rangle q^2)$ with the proton root-mean-square radius value $\langle r_p^2 \rangle^{1/2} = 0.80$ fm [26], then by the correction factor F_{CM} and in this way, using $B_2 = 0.298$ fm^2 and $d_2^2 = 0.298$ fm^{-2}, we can describe the electron data up to the momentum transfer squared q^2 of about 8 fm^{-2}. This form of F_2 is sufficient for our purpose because the maximum value of the transverse momentum transfer squared in the reaction (1) measured in experiment is about 3 fm^{-2} [5].

The transition density $\varrho_2(r)$ corresponding to form factor $F_2(q)$ equals

$$\varrho_2(r) = -\frac{8}{\sqrt{5}\pi} B_2 d_2^7 r^2 e^{-r^2 d_2^2}. \tag{25}$$

The ground state density distribution $\varrho(r)$ is taken from the harmonic oscillator shell model of the carbon

$$\varrho(r) = \frac{4}{A} \pi^{-3/2} R^{-3} \left(1 + \beta \frac{r^2}{R^2}\right) \exp(-r^2/R^2), \tag{26}$$

where R is the radius parameter and $\beta = (A-4)/6$.

Eqs (20, (23), (25) and (26) define the functions needed in the calculation of the production amplitude (14). The folded transition density distribution is approximately given by the expression

$$\tilde{\varrho}_{2M}(r) = -\frac{8}{\sqrt{5}\,\pi} B_2 c_2^7 r^2 e^{-r^2c^2_2} Y^*_{2M}(\Omega_r), \tag{27}$$

where

$$c_2 = (d_2^{-2}+2a)^{-1/2}. \tag{28}$$

The density $\tilde{\varrho}_{2M}(r)$ differs from $\varrho_{2M}(r)$ only in a new parameter c_2. In writing it we employ the fact that the amplitude for the inelastic electron scattering on not too heavy nuclei is in the impulse approximation

$$T(\vec{q}) = Zf(\vec{q})F_{fi}(\vec{q}). \tag{29}$$

In Eq. (29) $f(\vec{q})$ denotes the elastic electron-proton scattering amplitude and Z is the number of protons in the nucleus. The amplitude $f(\vec{q})$ depends on the three-dimensional momentum transfer $\vec{q}$. We would like to maintain the three-dimensional character of the Eq. (29), which is spoiled in the Glauber approximation valid at small scattering angles. In the Glauber approximation the longitudinal momentum transfer dependence of the amplitude is neglected. Therefore we restore it here, writing Eqs (27) and (28) in which the slope parameters $a/2$ and $1/4d_2^2$ of the amplitude $f_{12}(q^2)$ and inelastic form factor $F_2(q)$ enter in a symmetrical way. This does not mean, however, that we intend to apply our model to the description of the large-angle scattering; we are still restricted to rather small angles because the absorption factor of Eq. (12) posesses an eikonal character.

The absorption factor $G(\vec{b}, z)$, given by Eq. (12) can be rewritten in the following form:

$$G(\vec{b}, z) = G_{11}(b)H(b, z), \tag{30}$$

where

$$G_{11}(b) = \exp\{-(A-1)\int_{-\infty}^{\infty} dz \int d^2s\varrho(s, z)\gamma_{11}(\vec{b}-\vec{s})\} \tag{31}$$

and

$$H(b, z) = \exp\{-(A-1)\int_{z}^{\infty} dz' \int d^2s\varrho(s, z')\,[\gamma_{22}(\vec{b}-\vec{s})-\gamma_{11}(\vec{b}-\vec{s})]\}. \tag{32}$$

Let us note that if the elastic scattering amplitudes of the outgoing system 2 are the same as the incoming particle, $H(b, z) \equiv 1$ and the absorption factor equals $G_{11}(b)$. This is exactly the same absorption factor which should be considered in the inelastic scattering in which the incoming and outgoing particles are the same. This case is therefore a particular limit of our amplitude. The formulae presented below for the amplitude $T(q)$ might be used in the description of the inelastic scattering and in the production process with the

excitation of the same nuclear level. For completeness we quote here the analytical formulae for $G_{11}(b)$ and $H(b, z)$:

$$G_{11}(b) = \exp\left\{-\frac{A-1}{A}\frac{\sigma_1(1-i\alpha_1)}{2\pi(R^2+2a_1)}\times\right.$$

$$\left.\times 4\left[1+\frac{\beta}{2}+\beta\frac{2a_1}{R^2+2a_1}+\beta\frac{R^2}{R^2+2a_1}\frac{b^2}{R^2+2a_1}\right]e^{-\frac{b^2}{R^2+2a_1}}\right\}, \tag{33}$$

$$H(b, z) = \exp\left\{\frac{A-1}{A}\frac{1}{\pi}erfc\left(\frac{z}{R}\right)[u_1(b)-u_2(b)]+\right.$$

$$\left.+\frac{A-1}{A}\frac{1}{\sqrt{\pi}}\frac{z}{R}\beta e^{-\frac{z^2}{R^2}}[v_1(b)-v_2(b)]\right. \tag{34}$$

In Eq. (34) the functions u_j and v_j ($j = 1, 2$) are given by the following expressions:

$$u_j(b) = \frac{\sigma_j(1-i\alpha_j)}{R^2+2a_j}\left(1+\frac{\beta}{2}+\beta\frac{2a_j}{R^2+2a_j}+\beta\frac{R^2}{R^2+2a_j}\frac{b^2}{R^2+2a_j}\right)\exp\left(-\frac{b^2}{R^2+2a_j}\right), \tag{35}$$

$$v_j(b) = \frac{\sigma_j(1-i\alpha_j)}{R^2+2a_j}\exp\left(-\frac{b^2}{R^2+2a_j}\right) \tag{36}$$

and the error function

$$erfc(x) = \frac{2}{\sqrt{\pi}}\int_x^\infty e^{-t^2}dt. \tag{37}$$

In order to calculate the three-dimensional integral in Eq. (14) it is convenient to choose the cylindrical frame of coordinates: z, b, and azimuthal angle φ in the plane perpendicular to the z axis. As seen from the expressions (27) and (30), except for the exp $(i\vec{q}_T\vec{b})$ factor, only the harmonic wave functions $Y^*_{JM}(\Omega_r)$ depend on the angle φ. Integration over φ gives us the Bessel functions $J_M(q_T b)$. Next we use the relation $\sin\theta = b/(b^2+z^2)^{1/2}$ for the second argument θ of $Y_{JM}(\theta, \varphi)$ and finally we get the following expressions for the amplitudes $T_{2M}(\vec{q})$ devided by f_{12} $(m, 0)$:

$$F_{2,0}(\vec{q}) = -D\int_0^\infty dbbJ_0(q_T b)e^{-b^2c_2^2}G_{11}(b)\times$$

$$\times\int_{-\infty}^{\infty}dze^{iq_L z}(2z^2-b^2)e^{-z^2c_2^2}H(b, z), \tag{38}$$

$$F_{2,\pm1}(\vec{q}) = \pm iD\sqrt{6}\int_0^\infty dbb^2J_1(q_T b)e^{-b^2c_2^2}G_{11}(b)\times$$

$$\times\int_{-\infty}^{\infty}dze^{iq_L z}ze^{-z^2c_2^2}H(b, z), \tag{39}$$

$$F_{2,\pm 2}(\vec{q}) = D\sqrt{\tfrac{3}{2}} \int_0^\infty dbb^3 J_2(q_T b) e^{-b^2 c_2^2} G_{11}(b) \times$$

$$\times \int_{-\infty}^{\infty} dz e^{iq_L z} e^{-z^2 c_2^2} H(b, z). \tag{40}$$

In Eqs (38), (39) and (40) $D = 4A\,\pi^{-1/2} B_2 c_2^7$ and q_L is the longitudinal momentum transfer. At high energies and small scattering angles the values of the longitudinal momentum transfer may be approximated by its minimum value in the forward direction

$$q_L \approx q_{\min} = \frac{m^2 - m_1^2}{2p} + E^*, \tag{41}$$

where m_1 is the mass of the incoming particle, m is the effective mass of the produced system and E^* is the excitation energy of the nucleus.

Writing the Formulae (38)–(40) we neglect the Coulomb phase factor because ^{12}C is a light nucleus and we do not expect the Coulomb phase to play a very important role except, perhaps, in the diffractive minima of the angular distributions.

The double differential cross section for the production process, in which the spin alignment of the $^{12}C^*$ (4.4 MeV) nucleus is not measured, is given by the following relation

$$\frac{d^2\sigma}{dmdq_T^2} = \frac{d^2\sigma_N(m, 0)}{dmdq_T^2} |F(\vec{q})|^2. \tag{42}$$

The forward production cross section $d^2\sigma_N(m, 0)/dmdq_T^2$ on the nucleon is equal $|f_{12}(m,0)|^2$ and

$$|F(\vec{q})|^2 = \sum_{M=-2}^{2} |F_{2,M}(\vec{q})|^2. \tag{43}$$

4. Discussion of results

a. Angular distributions

In this chapter we present results of the numerical calculations of the angular distributions for the reaction (1). These distributions depend on a number of parameters describing the nuclear wave functions and the two-body amplitudes f_{11}, f_{22}, and f_{12}. To begin with, we discuss the most characteristic features of the factor $|F(q)|^2$ (Eq. (42)).

There are three nuclear parameters: B_2, d_2, defining the transition form factor (24), and the radius parameter R of the ground state density distribution (26). The radius R is fairly well determined from the elastic electron scattering experiments on carbon and we put $R = 1.6$ fm. The parameters B_2 and d_2 are not so well determined because the experimental study of the electron inelastic scattering is more complicated and the errors are larger than in the case of elastic scattering. The parameter B_2 gives only the normalization factor and the second parameter d_2 changes the shape of the angular distributions. Fig. 1 illustrates the characteristic shape of the nuclear factor $|F(q)|^2$ as the function of q_T^2, for a set of values d_2^2. The curves are calculated at the laboratory momentum $p = 6$ GeV$^2/c$

for the 3π effective mass $m = 1.1$ GeV and under the assumption that the amplitudes f_{22} and f_{11} are equal. The parmeters $\sigma_1 = 27.2$ mb, $\alpha_1 = -0.21$, and $a = 8.4$ GeV^{-2} are the average parameters of the known pion-proton and pion-neutron elastic scattering amplitudes at 6 GeV/c [27, 28]. The slope parameter a of the production amplitude is

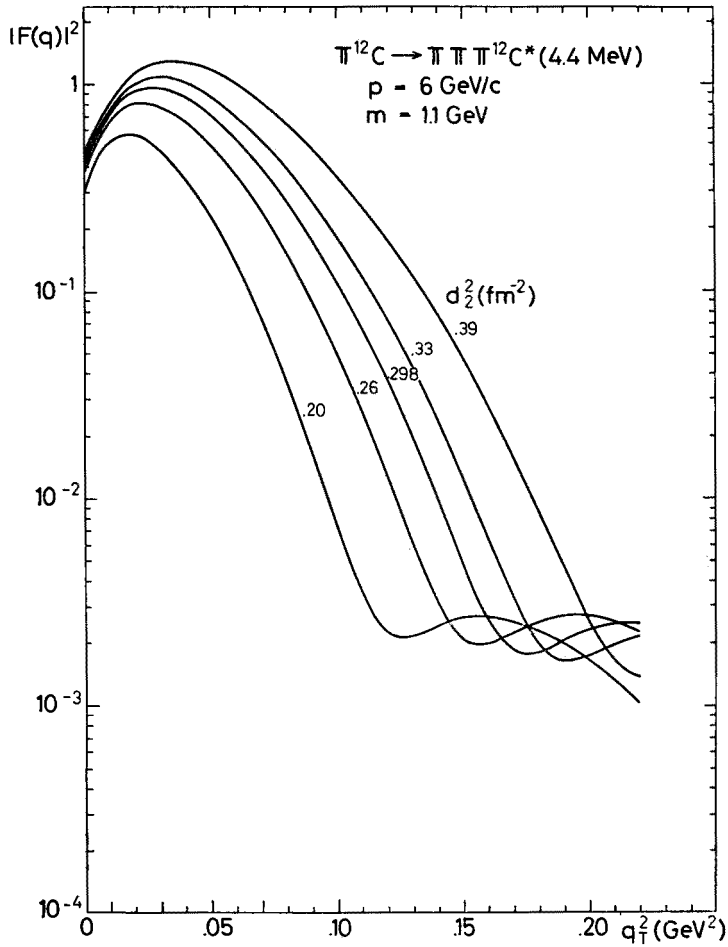

Fig. 1. Transverse momentum transfer squared dependence of the nuclear factor $|F(q)|^2$ given by Eq. (42) on the parameter d_2 of the transition density Eq. (25). For values of other parameters see text

taken equal to 10 GeV^{-2}. If not otherwise specified the above parameters are used for the amplitude f_{22} in the calculation of the curves shown in the next figures. We see from Fig. 1 that the curves have a dip in the forward direction followed by the broad secondary maximum and minimum, so the differential cross sections have a diffractive structure. This structure comes from the absorption of the incoming and outgoing particles. In the case of negligible absorption we do not get any minimum, choosing the inelastic form factor as in Eq. (24).

The effect of the absorption is shown in Fig. 2. The upper curve is calculated for the case of no absorption, the lower one for the 3π absorption equal to the single pion absorption. As seen from this figure, the absorption reduces the cross section at the maximum by a factor of about 2. This reduction has, however, the q_T^2 dependence, which is most clearly seen in the vicinity of the minimum at about 0.175 GeV^2.

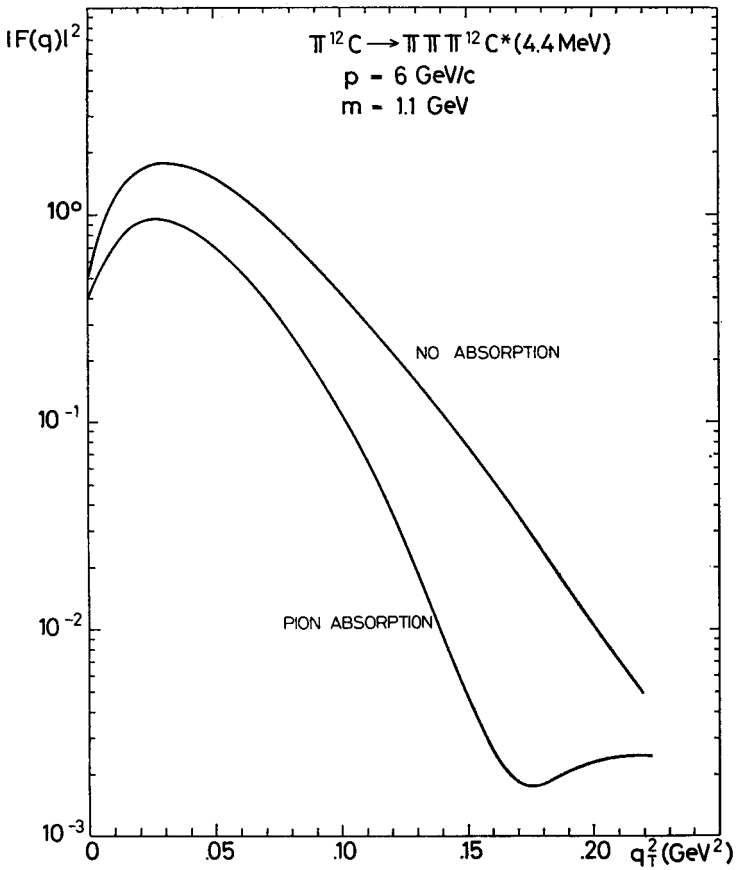

Fig. 2. Influence of the absorption on the momentum transfer distribution. Parameters for the upper curve are: $\sigma_1 = \sigma_2 = 0$, $\alpha_1 = \alpha_2 = 0$, $a_1 = a_2 = 0$ (no absorption) and for the lower curve: $\sigma_1 = \sigma_2 = 27.2$ mb, $\alpha_1 = \alpha_2 = -0.21$, $a_1 = a_2 = 8.4$ GeV^{-2} (pion absorption)

Figs 1 and 2 correspond to the production of the 3π mass $m = 1.1$ GeV. The angular distributions are very sensitive to the changes of the effective mass m. This is shown in Fig. 3 for $m = 0.5$, 1.1, 1.4, and 1.7 GeV. One can see a shift of the maximum to the left when the mass m increases; for 1.7 GeV the forward dip completely disappears and the maximum is in the forward direction. At the same time, the magnitude of the cross section decreases. This effect is caused by the factor $\exp(iq_L z)$ in the integrals (38), (39), and (40), which is related with mass m via the longitudinal momentum transfer q_L (Eq. (41)). The dependence of the angular distribution on the incoming particle momentum p at

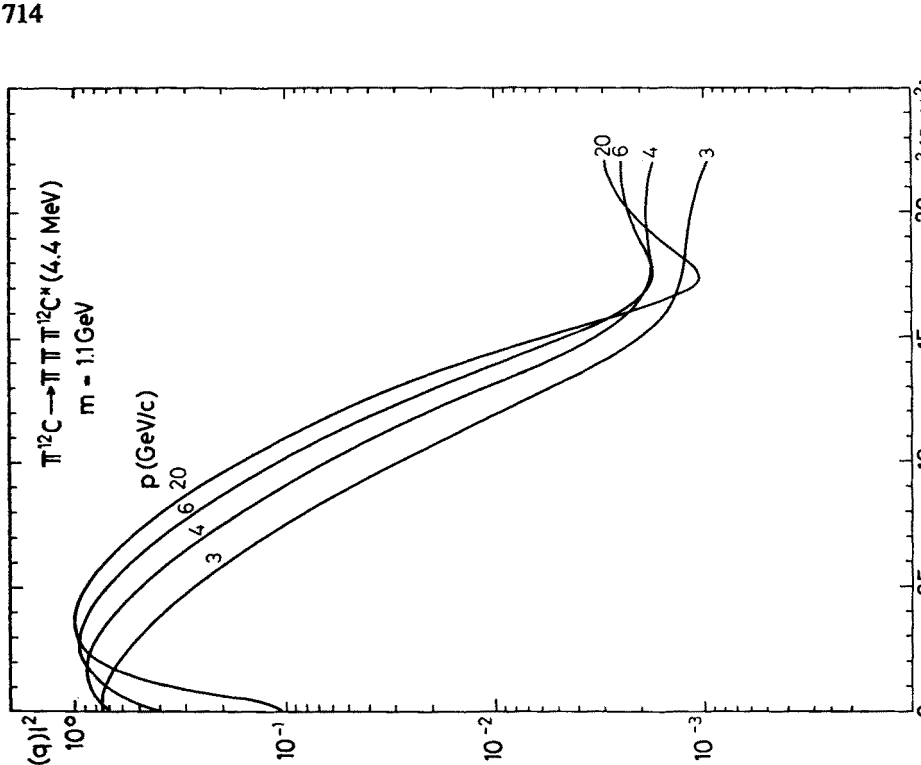

Fig. 3. Transverse momentum transfer squared dependence of the nuclear factor $|F(q)|^2$ for different produced masses m. The 3π absorption is assumed equal to the single pion one

Fig. 4. Transverse momentum transfer squared dependence of the nuclear factor $|F(q)|^2$ for different pion momenta at fixed $m = 1.1$ MeV. The 3π absorption is assumed equal to the single pion one

fixed m has the same origin. As we shall see later, the relations shown in Figs 3 and 4 have an important influence on the mass distributions and the energy behaviour of the integrated cross sections.

Now let us pass to the question how sensitive are the cross sections to the absorption of the outgoing system of produced particles. Here for the 3π production we compare four values of the ratio of the total cross section σ_2 to the pion-nucleon total cross section

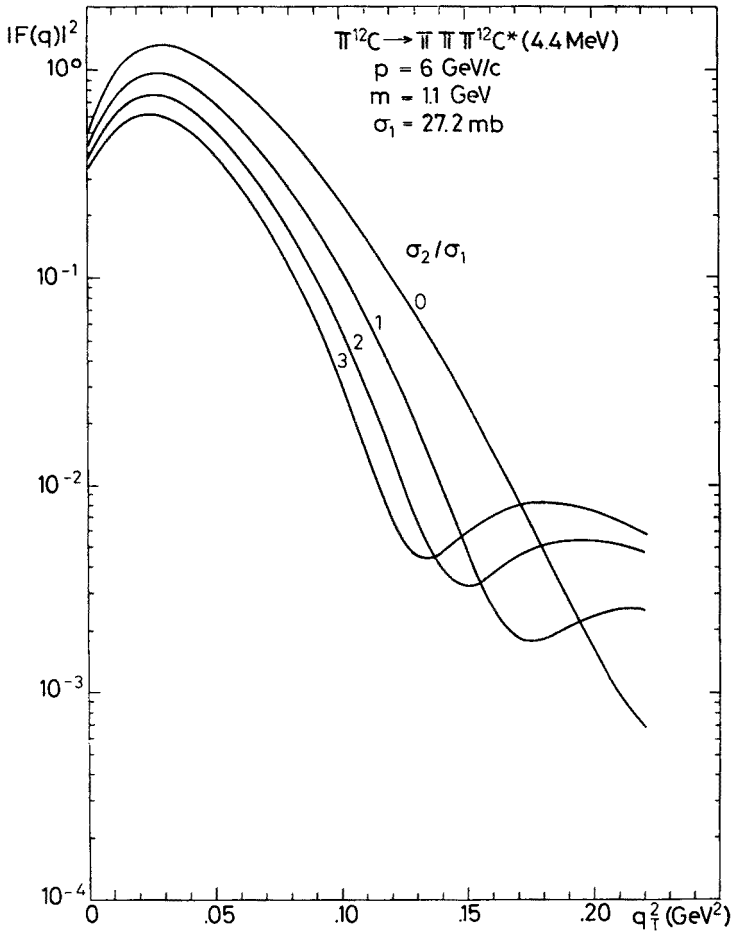

Fig. 5. Transverse momentum transfer squared dependence of the nuclear factor $|F(q)|^2$ for different ratios on the π-nucleon to the 3π-nucleon total cross sections. The 3π mass $m = 1.1$ GeV

σ_1. Figs 5 and 6 present the angular distributions for $m = 1.1$ and 1.7 GeV for $\sigma_2/\sigma_1 =$ $= 0$, 1, 2, and 3. In all cases we can observe that the absorption plays a more important role for the higher momentum transfers where it changes the position and depth of the minimum. For a comparison with the coherent production cross sections we have calculated similar curves for $m = 1.1$ GeV using the optical model formula of Ref. [29] (the

recoil factor is not included here). The curves are drawn in Fig. 7 for the same set of parameters as in Figs 5, 6. The angular dependence of the coherent process at the small momentum transfers is steeper than for the previous case, so the diffractive structure is shifted towards the smaller angles and is also very sensitive to the cross section σ_2. One can ob-

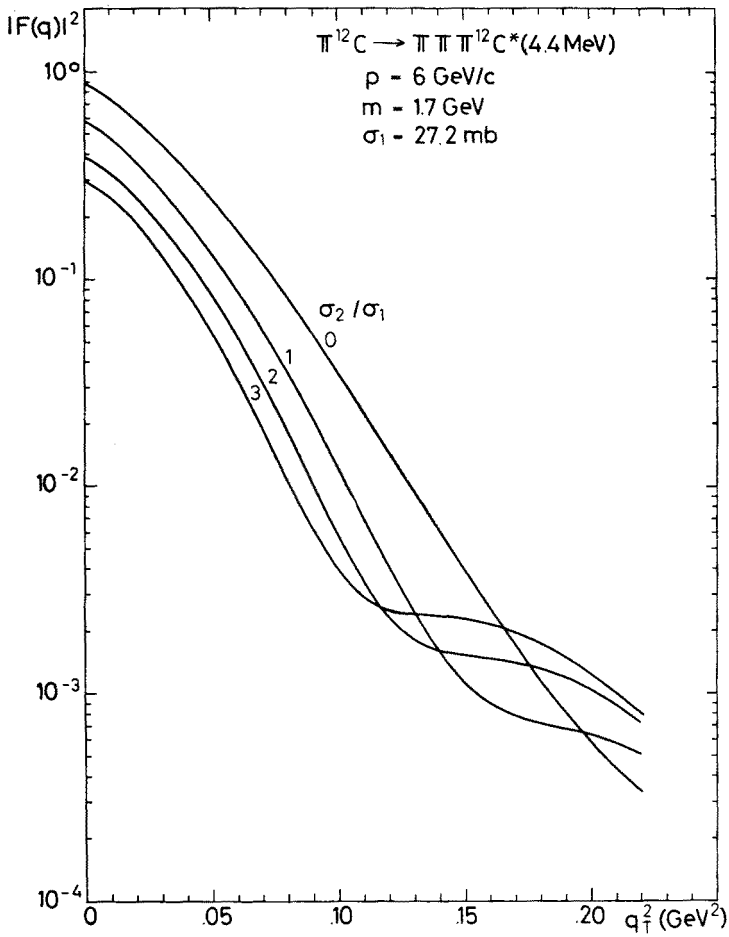

Fig. 6. The same dependence as in Fig. 5 but for $m = 1.7$ GeV

serve that the ratios of the distributions corresponding to the different values of σ_2 are larger for the coherent production case, although for the production with excitation of the nucleus the influence of the absorption is also quite important. This fact is connected with the spatial character of both processes governed by the transition density distributions. The coherent production process might happen in the whole volume of the nucleus while the production process with excitation of the nucleus rather in its surface part. Therefore the absorption of the outgoing pions from the centre of the nucleus is in the second case stronger than in the coherent production process, although in both cases the

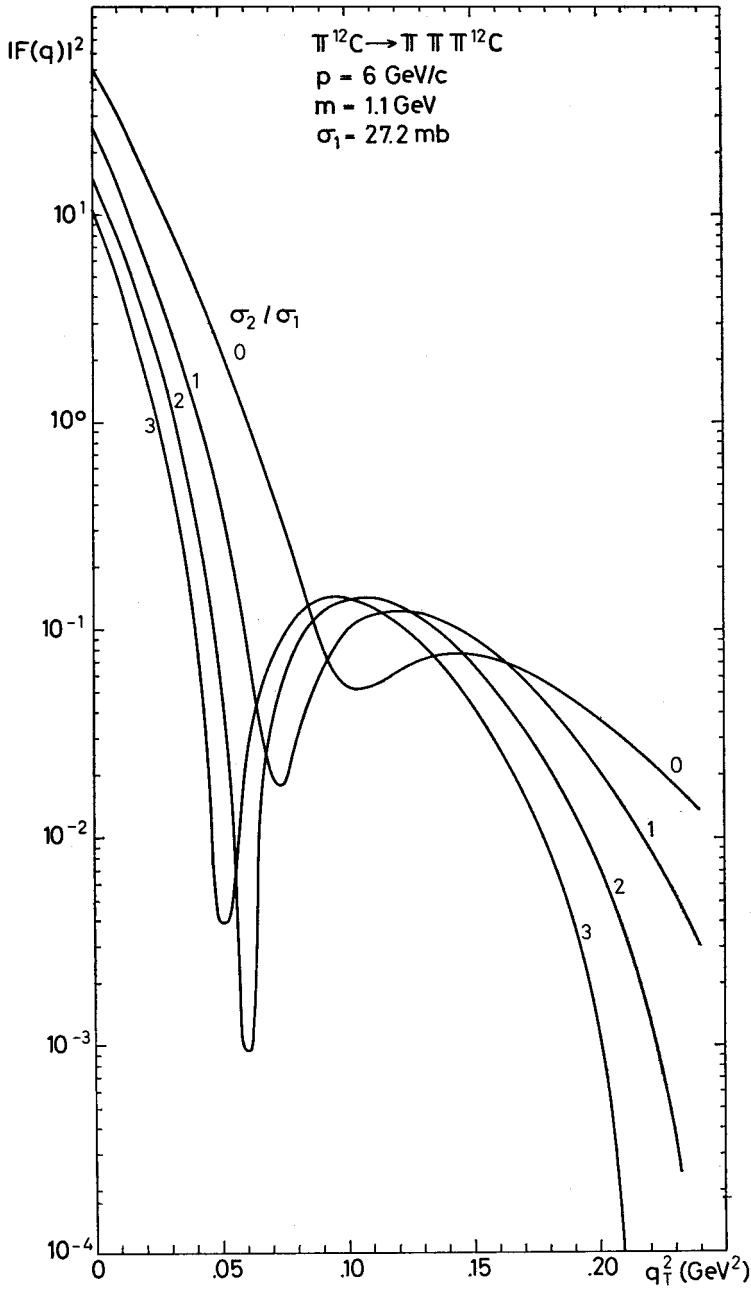

Fig. 7. Transverse momentum transfer squared dependence of the nuclear factor $|F(q)|^2$ for the coherent production at different ratios of σ_2/σ_1

flux of particles produced in the middle of the nucleus is considerably reduced by the nuclear absorption.

We have also studied the role of other two-body amplitude parameters. The ratio α_2 of the real to the imaginary parts of the f_{22} amplitude has a very weak influence on the shape and absolute magnitude of the differential cross section except for the vicinity of diffrac-

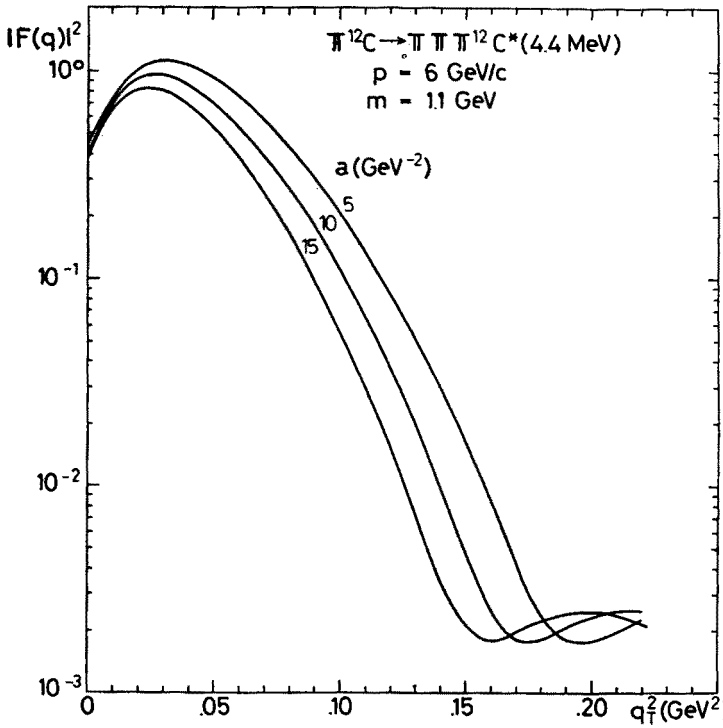

Fig. 8. Transverse momentum transfer squared dependence of the nuclear factor $|F(q)|^2$ for different values of the production amplitude slope a on a single nucleon. The 3π absorption is assumed equal to that of a single pion

tive minima. The same statement is true for the slope parameter a_2 when it is varied between 5 and 15 GeV^{-2}. The slope parameter of the production amplitude, however, plays a non-negligible role (see Fig. 8). This parameter is in our approach closely related with the parameter d_2 of the transition density distribution (Eg. (28)).

b. Mass distributions

The mass distributions can be obtained from Eq. (42) after integration over the momentum transfer squared:

$$\frac{d\sigma}{dm} = \frac{d^2\sigma_N(m, 0)}{dm dq_T^2} J(p, m), \tag{44}$$

where

$$J(p, m) = \int dq_T^2 |F(\vec{q})|^2. \tag{45}$$

They depend on the mass distribution produced on nucleons and on the integrated nuclear factor $J(p, m)$ whose mass dependence comes from the longitudinal momentum transfer. Let us first discuss some properties of this factor integrated over q_T. The integral depends on mass m and the incoming pion momentum p. The second relation is shown in Fig. 9 for $m = 1.1$ GeV. For $p \lesssim 7$ GeV/c we observe a quite strong increase in the factor

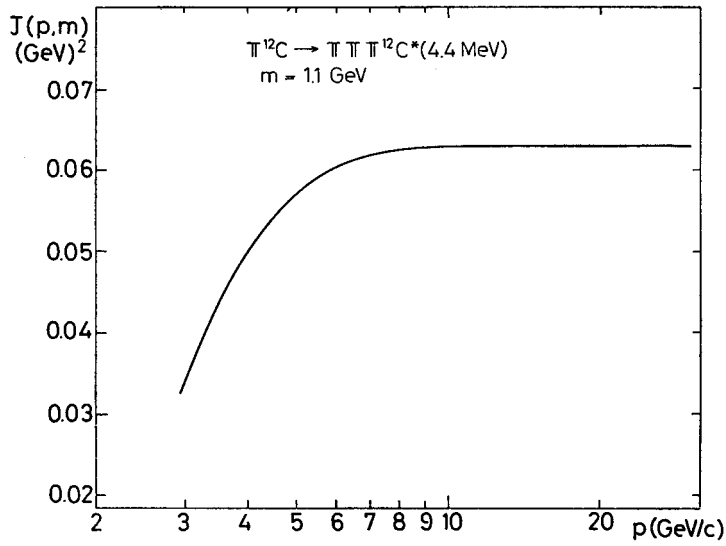

Fig. 9. Dependence of the integrated nuclear factor $J(p, m)$ given by Eq. (45) on the incoming pion momentum p. The 3π absorption equals that of a single pion and the produced mass $m = 1.1$ GeV

$J(p, m)$. The range of the momentum in which the factor $J(p, m)$ increases is wider for larger masses m. If the production cross section on nucleons does not decrease too strongly with energy the integrated over mass distribution cross section will increase similarly to the factor $J(p, m)$. This behaviour of integrated cross sections is identical to that in the coherent production cross sections, which increase with growing energy [29]. The mass dependence of the factor $J(p, m)$ for the different total cross section σ_2 is seen in Fig. 10. Production of higher masses is suppressed in comparison with small masses; for $m \geqslant 1$ GeV the curves fall steeply. From the same curves we can also read the relative magnitudes of the production cross section for a given mass m and the cross section σ_2. The curves presented in Fig. 10 have been obtained after integration of the angular distribution over the q_T^2 changing from 0 to 0.22 GeV^2.

c. Comparison with experiment

The preliminary data for the reaction (1) at 6 GeV have been published in Ref. [5]. In order to compare our model with these data we take the existing mass distributions of the reaction $\pi^-p \to \pi^-\pi^+\pi^-p$ at 5–7.5 GeV/c (shaded histogram in Fig. 2 of Ref. [30]) and assume that the slope parameter a equals 10 GeV^{-2} independently of m. The actual dependence of this parameter on the produced mass m is known from the experiments on

hydrogen (see for example Ref. [23]), but at the present experimental accuracy for the reaction (1) we do not expect that variation of this parameter with m is very important. We can use unnormalized cross section on hydrogen because the data of Ref. [5] are arbitrarily normalized. In our application we smooth by hand the mass distribution on

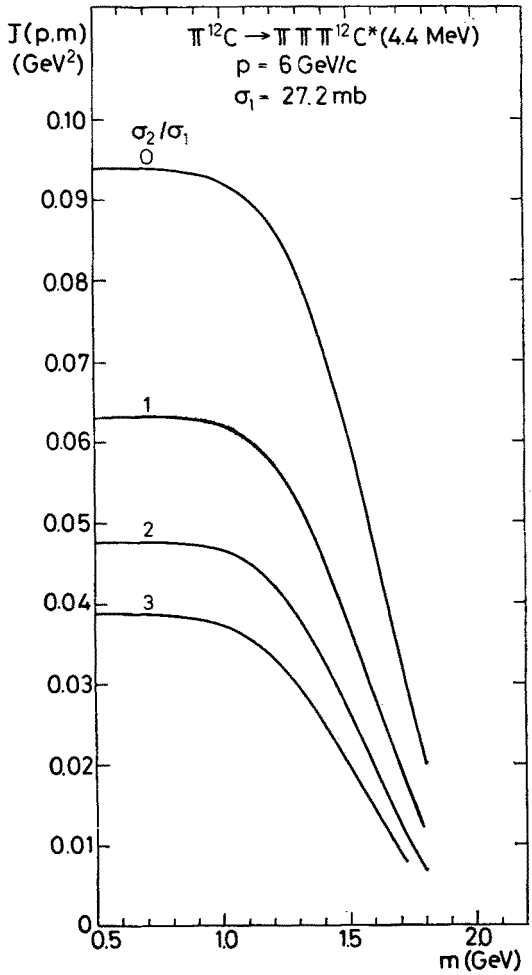

Fig. 10. Dependence of the integrated nuclear factor $J(p, m)$ on the produced 3π mass for different 3π-nucleon total cross-section σ_2

hydrogen from Ref. [30] and multiply it by the factor $J(p, m)$. In Fig. 11 our curve is compared with the experimental mass distribution of Ref. [5] (upper curve of Fig. 2b). A general agreement is obtained.

In Ref. [5] the transverse momentum transfer squared distribution for the 3π masses between 1.0 and 1.4 GeV is drawn. In Fig. 12 we compare it with our prediction. The experimental distribution is arbitrarily normalized as in Fig. 11 and its overall shape is reproduced by our curve under the assumption that the absorption of the 3π system is

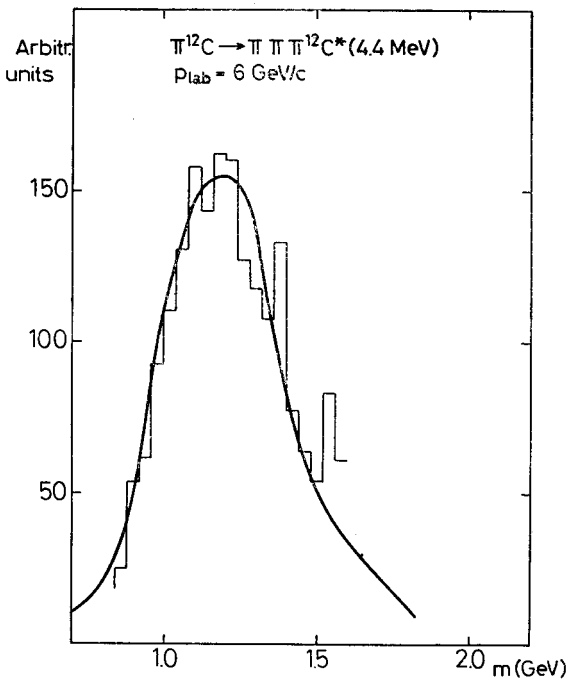

Fig. 11. Comparison of the experimental mass distribution from Ref. [5] with theory given by solid line

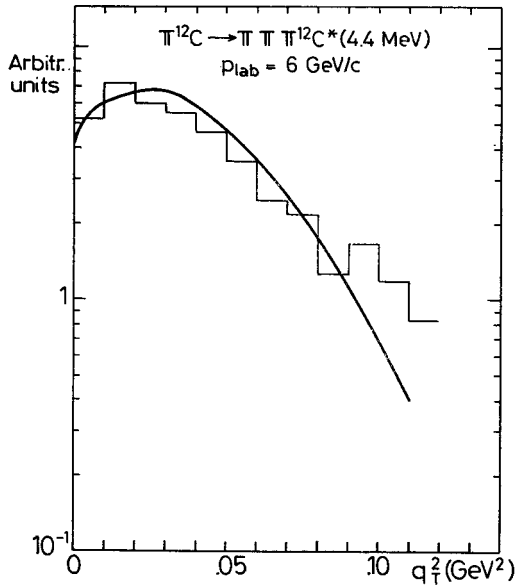

Fig. 12. Transverse momentum transfer squared distribution for the 3π mass range from 1.0 GeV to 1.4 GeV. Experimental histogram from Ref. [5] compared with the theoretical curve

the same as of a single pion, *Using these unnormalized data we cannot, however, exclude the possibility that the absorption of the outgoing pions is different from that of the incoming pions.* This is illustrated in Fig. 13, where the same angular distribution is drawn together with the four theoretical curves normalized to the same value at the maximum (calculated

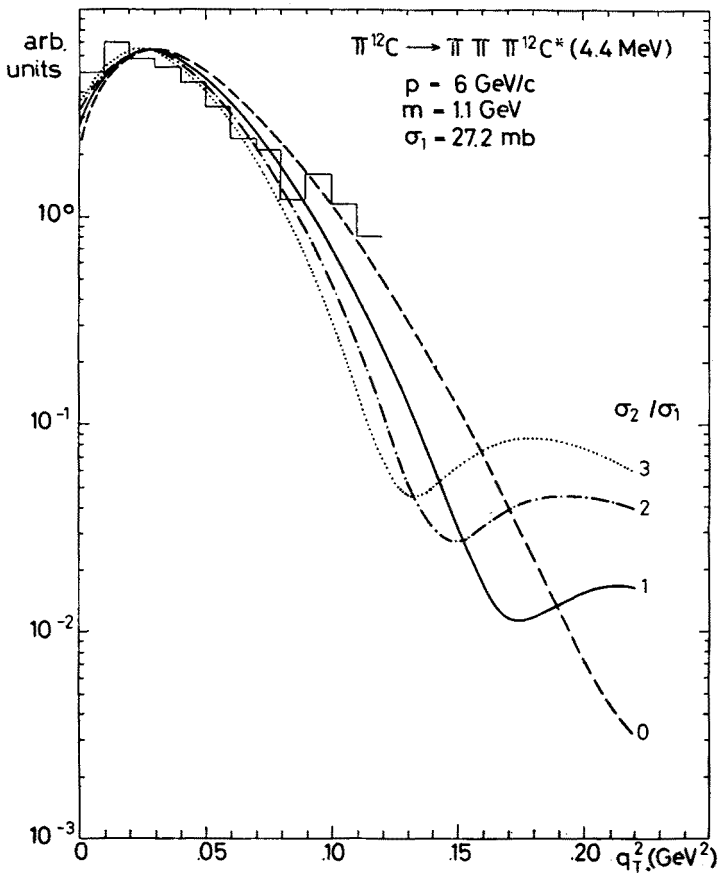

Fig. 13. Transverse momentum transfer squared distributions for different total cross sections σ_2 are compared with histogram taken from Ref. [5]. Theoretical curves are normalized to the same value at the maximum

for $m = 1.1$ GeV). It is clear that data of better quality and for larger momentum transfers are needed if we want to estimate the absorption of produced particles in the nucleus in that way.

5. *Conclusions*

The distorted wave impulse approximation compared with the preliminary data gives satisfactory results for the angular and the effective mass distributions for the reaction (1), provided one uses the transition densities obtained from the inelastic electron scattering

experiments. The present experimental data, however, are not sufficiently accurate to study in detail the absorption of the multipion system in nuclei and/or the possible use of nuclear production data as a source of the different parts of the *hadron-nucleon* production amplitudes. These aims may be achieved when *absolutely normalized data* confining the angular distribution at *larger momentum transfers* is accessible. Our analysis shows that the absorption of a group of particles changes not only the height of the maximum of angular distribution corresponding to the maximum of the transition form factor, but also changes the diffractive pattern of this distribution at larger production angles.

As in the coherent production process on nuclei, the process associated with excitation of a nucleus leading to the multihadron system having the large mass is suppressed in comparison with the production of the same mass on hydrogen. Therefore the production cross section obtained after the integration over the mass spectrum increases with incoming hadron momentum, although the corresponding cross section on hydrogen may be constant, or even slightly decreasing with energy. The effect comes from the longitudinal momentum transfer dependence of the nuclear amplitude.

In the DWIA model the same transition nuclear density may be used to describe the different processes leading to the excitation of the same nuclear level. This enables us to relate the experimental results of these processes in order to improve our parametrization of the transition density or to obtain some information about the hadron-nucleon amplitudes. One must remember, however, that this model neglects the correlations among the nucleons in the nucleus and the possible two — and more — step mechanism of excitation of nuclear levels. In general, the model describes well the shape of the angular distribution but in some cases discrepancies in the predictions of their absolute magnitude have been found. For example, in Ref. [15] the theory is 20% too high on the first maximum for the reaction $p^{12}C \to p^{12}C^*$ (4.4 MeV) [31] at 1 GeV, but as reported in Ref. [4] the theoretical curve gives a 2 times larger cross section at the maximum for the same reaction with pions at 4.5 GeV/c. We have checked these results, obtaining for our parametrization of the transition density in the first case about 35% to high value and exactly the same factor 2 in the second case. This situation needs further experimental and theoretical studies, especially for the case of the pion inelastic scattering.

Note added in proof:

In the present paper the terms corresponding to the case when the production and excitation take place on different nucleons are omitted. They are discussed by one of us (L.L.) in his talk given at the International Meeting on Hegh Energy Collisions Involving Nuclei, Trieste, 9–13 September 1974 (to be published in the Proceedings of this Conference).

REFERENCES

[1] H. H. Bingham, invited talk presented at the Fifth International Conference on High Energy Physics and Nuclear Structure, Uppsala, Sweden, 18–22 June 1973.
[2] C. Bemporad et al., *Nucl. Phys.* **B33**, 397 (1971).
[3] D. Scipione et al., *Phys. Lett.* **42B**, 489 (1972).
[4] J. L. Groves et al., *Study of the reaction* $^{12}C(\pi, \pi)^{12}C^*$ *at* 4.5 *GeV*, contribution to the Fifth Interna-

tional Conference on High Energy Physics and Nuclear Structure, Uppsala, Sweden, 18–22 June 1973.
[5] G. Ascoli et al., *Phys. Rev. Lett.* **31**, 795 (1973).
[6] L. Stodolsky, *Phys. Rev.* **144**, 1145 (1966).
[7] C. Rogers, C. Wilkin, *Lett. Nuovo Cimento* **1**, 575 (1971).
[8] J. F. Germond, J. P. Amiet, *Comparative analysis of pion-nucleus elastic and inelastic scattering, preprint*, Institut de Physique de l'Université Neuchâtel (1973).
[9] Y. Alexander, A. S. Rinat, *Phys. Lett.* **45B**, 190 (1973).
[10] Y. Alexander, A. S. Rinat, *Ann. Phys.* **82**, 301 (1974).
[11] J. L. Friar, *Particles and Nuclei* **5**, 45, (1973).
[12] V. E. Starodubsky, O. A. Domchenkov, *Phys. Lett.* **42B**, 319 (1972).
[13] V. E. Starodubsky, *Nucl. Phys.* **A219**, 525 (1974).
[14] G. Nixon, Lawrence Berkeley Laboratory *preprint*, LBL-1769 (1973).
[15] J. Saudinos, C. Wilkin, CERN *preprint* TH 1808 (1974), to be published in *Annual Review of Nuclear Science*, vol. 24 (1974).
[16] R. J. Glauber, *Lectures in Theoretical Physics*, vol. I, ed. by W. E. Brittin et al, Intersc. Publ., New York 1959.
[17] W. Czyż, *Advances in Nuclear Physics*, vol. 4, ed. by M. Baranger and E. Vogt, Plenum Press, London–New York (1971.
[18] K. S. Kölbig, B. Margolis, *Nucl. Phys.* **B6**, 85 (1968).
[19] H. H. Bingham, in *Proceedings of the Topical Seminar on Interactions of Elementary Particles with Nuclei*, Trieste (1970).
[20] W. Beusch, *Acta Phys. Pol.* **B3**, 679 (1972).
[21] C. Bemporad et al., *Partial wave analysis of the 3π states coherently produced on nuclei*, paper No 215 submitted to the Aix-en-Provence International Conference on Elementary Particles (1973).
[22] H. Überall, *Electron Scattering from Complex Nuclei*, part B, Academic Press, New York and London 1971.
[23] J. V. Beaupre et al., *Phys. Lett.* **41B**, 393 (1972).
[24] H. Crannell, *Phys. Rev.* **148**, 1107 (1966).
[25] L. Leśniak, H. Wołek, *Nucl. Phys.* **A125**, 665 (1969).
[26] R. Herman, R. Hofstadter, *High Energy Electron Scattering Tables*, Stanford Univ. Press, Stanford, California 1960.
[27] G. Höhler, R. Strauss, *Tables of pion-nucleon forward amplitudes*, University of Karlsruhe *preprint*, October 1971.
[28] T. Lasinski, R. Levi Setti, B. Schwarzschild, P. Ukleja, *Nucl. Phys.* **B37**, 1 (1972).
[29] H. Leśniak, L. Leśniak, *Phys. Lett.* **34B**, 135 (1971).
[30] G. Ascoli et al., *Phys. Rev.* **7D**, 669 (1973).
[31] R. Bertini et al., *Phys. Lett.* **45B**, 119 (1973).